Rodríguez-Rodríguez, H.; Acebrón, M.; Juárez, B.; Arias-Gonzalez, JR. (2017). Luminescence Dynamics of Silica-Encapsulated Quantum Dots During Optical Trapping. The Journal of Physical Chemistry C. 121(18):10124-10130. https://doi.org/10.1021/acs.jpcc.6b11867

Luminescence Dynamics of Silica Encapsulated Quantum Dots During Optical Trapping

Héctor Rodríguez-Rodríguez,[1,2] María Acebrón,[1] Beatriz H. Juárez[1,2] and J. Ricardo Arias-Gonzalez[1,3*]*

[1]Instituto Madrileño de Estudios Avanzados en Nanociencia (IMDEA-Nanoscience), 28049 Cantoblanco, Madrid, Spain

[2]Departamento de Química-Física Aplicada, Universidad Autónoma de Madrid, 28049 Cantoblanco, Madrid, Spain

[3]CNB-CSIC-IMDEA Nanociencia Associated Unit "Unidad de Nanobiotecnología", 28049 Cantoblanco, Madrid, Spain.

ABSTRACT: The trade-off between photo-brightening and photo-bleaching controls the emission stability of colloidal quantum dots. This balance is critical in optical trapping configurations, where irradiances that confine and simultaneously excite the nanocrystals in the focal region cannot be indefinitely lowered. In this work, we studied the photo-brightening and bleaching behaviors of two types of silica-encapsulated quantum dots excited upon two-photon absorption in an optical trap. The first type consists of alloyed CdSeZnS quantum dots covered with a silica shell. We found that the dynamics of these as-prepared architectures are similar to those previously reported for bare surface-deposited quantum dots, where thousands of times smaller irradiances were used. We then analyzed the same quantum dot systems treated with an extra intermediate sulfur passivating shell for the better understanding of the surface traps influence in the temporal evolution of their emission in the optical trap. We found that these latter systems exhibit better homogeneity in their photodynamic behavior compared to the untreated ones. These features strengthen the value of quantum dot preparations in

optical manipulation as well as for applications where both long and maximal emission stability in physiological and other polar media are required.

Introduction

Colloidal semiconductor nanocrystals or quantum dots (QDs) have evolved from mere materials science outsiders in biology and medicine to essential tools for imaging, sensing and diagnostics, besides their potential applications in photovoltaics or quantum computing, due to their unique optical properties.

Recently demonstrated simultaneous optical trapping (OT) and excitation of QDs has enriched the applications of these fluorescent probes. OT of a nanoparticle (NP) can be just generated by tightly focusing a laser beam near an object with majorly dielectric behavior at a specific laser wavelength.[1-3] The electromagnetic field of the beam induces a time-dependent dipole within the NP volume with a concomitant attractive force pointing to the center of the focal region, where the field intensity is the highest.[4-5] OT of QDs has been demonstrated by Pan et al. using a 1047 nm picosecond laser[6] and has also been reported by Jauffred et al. with a 1064 nm continuum-wave trapping beam.[7-8] This method has been found to be convenient in water because this medium minimizes heating effects stemming from optical absorptions.[9] Recently, silica-encapsulated (QD@SiO_2) and other polymer-encapsulated QDs have been trapped in nano-plasmonic structures.[10] These systems present several advantages in a wealth of cutting-edge applications[11-12] and may preserve optical properties.[13]

Photoluminescence (PL) of optically excited colloidal QDs may suffer from a variety of non-reversible photo-induced effects, including brightening, bleaching and blueing. Photo-brightening consists of an enhancement in the PL intensity, presumably due to surface traps passivation,[14-16] although many others mechanisms such as ligand degradation have also been proposed.[17] In contrast, the formation of inter-band recombination centers induces the progressive quenching of the PL, giving rise to the photo-bleaching effect.[18-19] Spectral blueshift is associated to the reduction of the effective emitting volume, usually another consequence of the photo-oxidation of the QD surface. Heat-assisted diffusion of atoms within the QD structure has also been recently proposed as a source of blueshift in some QDs.[20-21] Since the aforementioned phenomena may take place simultaneously, there is a trade-off between light-assisted lightening and dimming processes.

Compared to core/shell or core/shell/shell QDs exhibiting an abrupt and defined interface, alloyed QDs, where there is a graded composition of elements from the inner core to the outer shell, show better photochemical stability and even show suppression of undesirable blinking in single particle experiments.[21-22] The burst of research lines involving OT of QDs demands studies on photodynamic effects at the laser beam focus, which to the best of the authors' knowledge, have not been performed in detail. The origin and nature of these effects have shown to be highly dependent on the medium surrounding the QD,[23-24] hence the characterization of optically-confined QDs, both at the single-particle level or in clusters, is gaining interest, especially for molecular and cell biology.

In the following, we show that an extra sulfur-passivizing shell improves the emission stability of silica-encapsulated CdSeZnS QDs in a laser trap. Our results further validate optical tweezers for the study of the emission dynamics of QDs in solution, despite the typical irradiances in the trapping focus are significantly larger than those used in experiments where the QDs were deposited on a surface.

Experimental section

QD synthesis

The synthesis and further SiO_2-coating of alloyed CdSeZnS QDs have been performed according to our previous report.[20] Surface treatment was carried out by sulfur addition to the initial QD microemulsion before SiO_2-coating. The sulfur precursor was in turn prepared in microemulsion maintaining the ratio surfactant/water/organic-solvent and the amount of sulfur for a controlled formation of the passivation monolayer was calculated according to the SILAR methodology.[25] Ethanol dispersions of QD@SiO_2 were sonicated before being flowed in a microfluidic chamber for the optical trapping experiments (see below). The morphology of QDs and QD@SiO_2 was characterized by transmission electron microscopy (TEM) using a JEOL JEM 1010 microscope operating at 100 kV. Average size values were obtained from the TEM images, measuring at least 100 particles. PL spectra of QDs microemulsions were recorded in a spectrofluorometer (Horiba JobinYvon Fluoromax-4) using an excitation wavelength of 420 nm.

Optical trapping configuration and irradiance

Our instrument is a dual, counter-propagating beam optical trap in which two oppositely travelling laser beams in the near-infrared (835 nm) are focused inside a microfluidics chamber by two each microscope objectives (Nikon CFI plan-Apochromat 60X, NA=1.2).[26] Deflections in the trapping beams are measured by two position-sensitive photodetectors (PDs). Numerical aperture of the trapping lasers

was NA ≈ 0.4. Based on paraxial Helmholtz approximation for a Gaussian beam, beam waist was estimated to be $2w_0 \approx 1.3$ μm and total trapping power was set to 90 mW at the focal region. The resulting irradiance in the trap is $\approx 6.3\times10^{3}$ kW cm^{-2}. The generated PL was collected through one of the objectives and redirected to both a spectrometer (Ocean Optics USB2000+) and a CCD camera for monitoring purposes.

Thermal noise and Stokes' law size determination

To measure the hydrodynamic size of the optically trapped specimens, we followed previously developed methods based on the analysis of the friction coefficient,[9, 27-28] which we summarize next: In the thermal noise method, force fluctuations of a trapped particle in a direction perpendicular to the optical axis were obtained from the voltage signal in the PDs operating at 100 kHz during 5.24 s. The time interval was divided into 128 sub-intervals of 40.96 ms. Next, force fluctuations (in voltage units) in each interval were Fourier transformed in the time domain (–∞, +∞) and averaged over the 128 samples. The resulting data (in voltage squared per hertz units) were fitted to the equilibrium power spectrum density (PSD) of an overdamped particle in a harmonic potential, yielding the so-called corner frequency, f_c, and drag coefficient, γ, as parameters (see also the main text). In order to transform volts to force units, the same procedure was applied to polystyrene (PS) beads of known size (Polybead Polyscience, 1-μm diameter). In the Stokes' law method, the micro-fluidic chamber was displaced transversally to the optical axis using a translation stage (Thorlabs MDT-631) while a particle was in the trap. Drag velocity was determined by recording chamber displacements using an LVDT sensor (Schaevitz PCA 116-100) as a function of the time. The drag coefficient, γ, was extracted from the fitting to $F = -\gamma v$. For reference experiments, we used PS microspheres with two other nominal diameters (as provided by the vendor): 0.53 and 2.23 μm (Spherotech).

Results and discussion

Alloyed CdSeZnS QD@SiO_2 were prepared in microemulsion (QD@SiO_2)[20] along with an extra sulfur-passivated version of these structures (pQD@SiO_2), see Experimental Section. The extra sulfur

shell improves the robustness of the QD PL, as it will be further shown. Its selection was made on the basis of previous XPS analysis evidencing an outer Zn-rich shell, which unsaturated atoms could act as surface traps leading to non-radiative pathways with subsequent quenching of the PL. Fig. 1 shows the sample characterization. The extra sulfur shell yielded hardly appreciable changes in the mean and spread of the size distributions (Fig. 1a, b and c). Sulfur passivation and silica encapsulation did not either significantly changed the PL peak wavelength (Fig. 1d, e and f). The similarity between the two preparations, both in size and in emission spectrum, made possible to perform a rigorous quantitative comparison between their photodynamics.

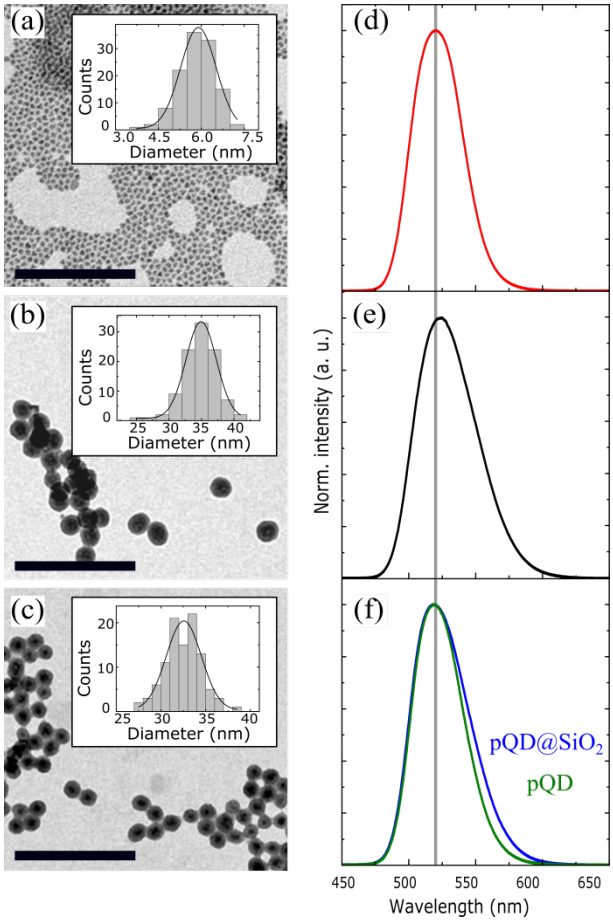

Figure 1. Sample characterization. TEM images of, (a), QD cores, (b), QD@SiO_2 and (c) pQD@SiO_2. Scale bars, 200 nm. Insets, size statistical distributions. Black curves, Gaussian fits yielding diameters (mean ± HWHM) of 5.9 ± 0.7 nm, 34.7 ± 2.6 nm and 32.5 ± 2.0 nm for QD, QD@SiO_2 and pQD@SiO_2, respectively. Photoluminescence (PL) of, (d), QD cores, (e), QD@SiO_2 and, (f) pQD@SiO_2 as obtained in water-in-oil microemulsion. In (f), the PL from the QD cores with the passivating S layer is shown in green whereas that from these particles after SiO_2 encapsulation is shown in blue. The grey vertical line in the right panels is a guide to the eye marking the PL peak wavelength of the original QD cores.

We manipulated both QD@SiO_2 and pQD@SiO_2 in an optical tweezers setup, see Fig. 2 and Experimental Section, as earlier applied for the manipulation of single nanostructures that manifest a time-dependent dynamics.[9, 27-28] A colloidal dispersion of QDs in ethanol was flowed into the microfluidics chamber for their trapping. Under our experimental conditions, QDs in the focal region bunched in small groups of QDs (QD clusters from now on)[29] and were therein excited by a two sub-bandgap photon absorption process.[7, 30] Since the period between two trapping episodes can be statistically lengthened by lowering the QD concentration pumped into the microfluidics chamber, it was possible to maintain isolated QD clusters in the trap for minutes.

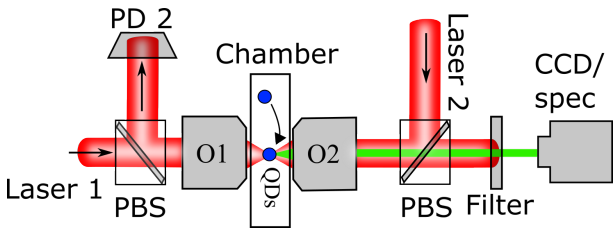

Figure 2. Simplified experimental setup. Two near-IR laser beams are focused through objective lenses (O1 and O2) after passing through other optical elements, including polarizing beam splitters (BS) like the represented one that transmit the visible range by polarization. Scattered intensity is analyzed by position sensitive photodetectors (PD). Only the PD that registers the deflections of laser 2 is shown for the sake of simplicity. Luminescence from the trap is collected through O2 and visible-pass filtered for both CCD camera image and spectrometer analysis (not including near-IR wavelengths). Trapping of QD clusters takes place in a microfluidic chamber.

Behavior of the QD clusters in the optical trap

The hydrodynamic diameter of the trapped clusters was determined by means of the thermal noise analysis. The equilibrium power spectrum density (PSD) of an overdamped particle in a harmonic potential is:

$$\langle \Delta F^2(f) \rangle_{eq} = 2\gamma k_B T \frac{f_c^2}{f^2 + f_c^2}, \quad (1)$$

where the brackets represent the equilibrium ensemble average, γ is the drag coefficient, $f_c = \kappa/2\pi\gamma$ the corner frequency (in Hz), k_B the Boltzmann constant, T the temperature, f the sampling frequency (in

Hz) and κ the spring constant accounting for the stiffness of the optical trap. Data sets of force vs. time are transformed into the frequency domain, as explained in the experimental section, and fitted to Eq. (1), yielding values for the free parameters γ and f_c. Then, the effective diameter, $d = \gamma/3\pi\eta$, of a sphere hydrodynamically equivalent to the trapped cluster is derived, being η the viscosity of the medium. Measured PSDs for a typical QD@SiO_2 cluster and a 1-μm PS bead are shown in Fig. 3 (*a*). These transformed data normally display artefactual electronic noise above ~10^3 Hz related to the acquisition system.

Hydrodynamic diameters were alternatively measured by means of the Stokes' law (see the experimental section and Fig. 3 (b)), yielding similar values to those obtained via PSD measurement, as shown in Fig. 3 (c). Cluster size generally varies from 0.5 to 1.5 μm while most probable diameter is near 1 μm, Fig. 3 (*d*). An upper limit for the number of QDs in a typical cluster can be set at ~10^3 from the close packaging model.[31] Nevertheless, in TEM pictures (Fig. 1 (b) and (c)), QDs fill a 50% of planar cluster images, yielding a QD density of 37%. Then, from both the hydrodynamic size analysis and the TEM images the number of QDs is estimated in ~10^2. The fact that we observed clusters in the trap within this estimation in the number of NPs is further supported by the inhomogeneous broadening of the registered emission spectra (see Supplementary Information for details).

Fig. 3 (e) shows the dependence of κ (transversal to the optical axis) on the hydrodynamic diameter for QD@SiO_2 clusters. Within the size range found in our sample, κ increases with diameter since it does not exceed the transversal dimensions of the beam waist at the laser focus (see the experimental section and [32-33]). In fact, κ measured for 2.23 μm PS beads is similar to that found for 1.0 μm PS beads, indicating a focal region with transversal size within these values. PS beads exhibited higher κ owing to the higher refractive index of polystyrene with respect to the effective refractive index of a QD cluster, which is in the end an overall mixture of QD cores, silica and dispersive medium.

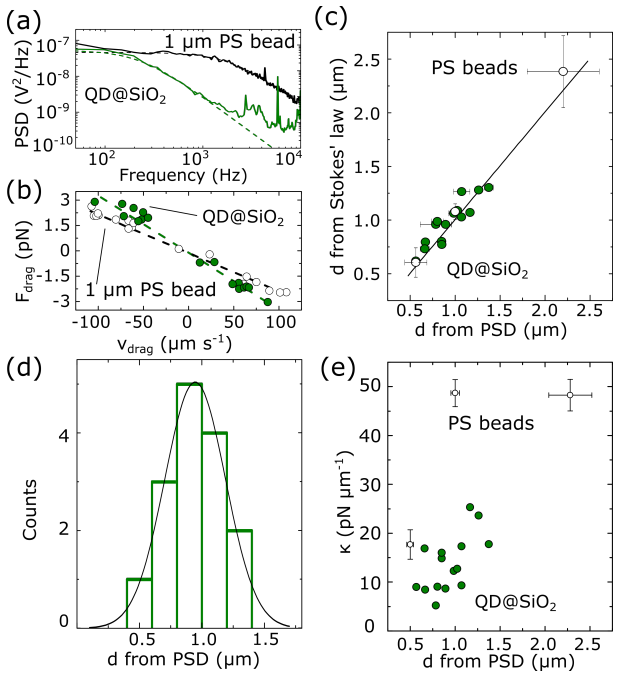

Figure 3. Cluster size analysis in the optical trap. (a) PSD measurements of a typical QD@SiO_2 cluster (green) and a 1-μm diameter PS bead (black). Dashed curves represent the fit of Eq. (1) to the experimental data with corner frequencies at 226 ± 9 Hz and 1941 ± 28 Hz, respectively, for these particular samples. Estimated sizes from this analysis yielded 1.07 ± 0.02 μm for the represented QD@SiO_2 cluster and 1.00 ± 0.01 μm for the bead. (b) Drag force versus velocity for a QD@SiO_2 cluster of similar size (green dots) and a PS bead (hollow dots). Dashed lines are linear regressions to the experimental data, yielding diameters of 1.53 ± 0.06 μm for the represented cluster and 1.10 ± 0.07 μm for the bead. (c) Comparison of hydrodynamic diameters obtained via Stokes' law and PSD on both QD@SiO_2 clusters (green dots) and PS beads (hollow dots). The black line is a guide to the eye showing the points where both sizes equal. (d) Size distributions derived from PSD analysis of QD@SiO_2 clusters; black curve, normal distribution fitting the data histograms ad yielding mean and standard deviations of 0.95 ± 0.49μm. (e) Transversal trapping stiffness as a function of the particle size for QD@SiO_2 clusters (green dots) and PS bead of three diameters (hollow dots).

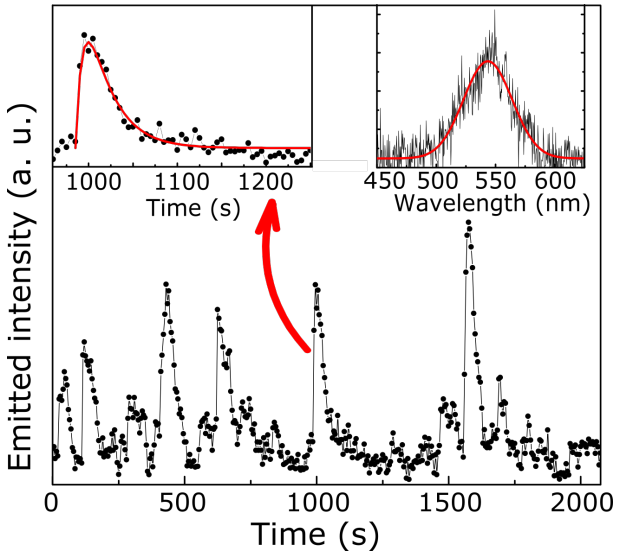

Figure 4. Typical temporal evolution of the luminescence generated in the optical trap. Each intensity peak indicates a trapping event of a QD@SiO_2 cluster. Left inset, luminescence temporal behavior during one of the trapping events, as marked by the red arrow. CER model (Eq. (2)) has been fit to the experimental data (red curve) yielding $k_a = 0.12 \pm 0.02$ s^{-1} and $k_d = 0.036 \pm 0.004$ s^{-1} for this particular measurement. Right inset, emission spectrum at one specific instant within that trapping episode. Red curve, Gaussian fit yielding peak emission at 543.5 ± 20.5 nm (mean ± HWHM).

Photodynamics of the optically trapped QD clusters.

The PL coming from the optically trapped sample evolves as shown in Fig. 4 in a typical OT experiment: The incorporation of a QD cluster is revealed by a rapid increase in the PL intensity, or activation, as previously reported for other nano-sized luminescent particles.[29] QD clusters then show a photo-brightening enhancement of the PL followed by a slow decay distinctive of photo-bleaching. Emission spectra at specific instants were recorded using an integration time of 5 s. A representative spectrum of a trapped QD@SiO_2 cluster is shown in the right inset of Fig. 4. As further analyzed in the Supplementary Information, the collected intensity exhibits inhomogeneous broadening due to the spread of QD sizes in the trap.

The temporal profile of the PL intensity (activation, enhancement and decay) is given by a consecutive elementary reaction (CER) model proposed by Lee and Osborne in terms of populations of emitting QDs.[34] The collected intensity, $I(t)$, can be assumed to be proportional to the number of emitting particles:

$$I(t) = A_0 \frac{k_a}{k_d - k_a}(e^{-k_a t} - e^{-k_d t}) + B_0 e^{-k_d t}, \quad (2)$$

where A_0 and B_0 are the initial intensities of the dark and fluorescent fractions of QDs, respectively, whereas k_a and k_d are the characteristic photo-brightening and photo-bleaching rates, respectively. This proportion has been found linear in Ref. [34] for small populations of emitting nanoparticles but remains useful when bulk samples are considered.[35-36] Eq. (2) fitted properly the experimental data, as shown in left inset, Fig. 4.

Since QD clusters are firmly bunched electrostatically during the experiment and our setup allows a fine control of the QD cluster concentration, other phenomenologies such as an exchange of QDs between the trapped cluster and the medium[37] have been discarded. For a given sample, we collected intensity traces for individual clusters. Each cluster was maintained in the optical trap until decaying emitted intensity was comparable to detector noise level, as shown by the multi-peak intensity profile in Fig. 4. Then, the nearly bleached cluster was released from the trap. QD cluster concentration was tuned to avoid multi-step, cumulative trapping events during the recording of an intensity profile. However, the co-existence in the optical trap of several emitting clusters at a time, each bearing a characteristic CER-predicted profile, was sometimes observed (see Supplementary Information). In order to keep systematical experimental conditions, values coming from these multi-trapping experiments have been excluded from the analysis.

Statistical distributions of k_a and k_d measured over a representative number of QD@SiO_2 and extra passivated pQD@SiO_2 clusters are shown in Fig. 5. QD@SiO_2 clusters are observed to activate faster (higher k_a) than pQD@SiO_2, Fig. 5 (*a*) and (*b*), respectively, thus suggesting that the intermediate extra S shell tempered the PL enhancement. The extra S layer certainly made pQD@SiO_2 clusters less sensitive to the light-induced phenomena that limit the stability of their emission, probably by ridding surface defect states which normally stem from surface trap neutralization.[14, 24] In fact, averaged k_d from QD@SiO_2 is considerably higher than that from pQD@SiO_2, Fig. 5 (*c*) and (*d*), respectively. The behavior of k_d is more specifically related to the shielding effect that generates the extra passivation layer against oxygen, thus delaying photo-oxidation processes on the surface of the QD cores.[38-39] It is also observed that QD@SiO_2 clusters exhibit a much wider k_d distribution, hence a much less homogeneous behavior, than pQD@SiO_2 ones (compare Figs. 5(*d*) and (*b*)). Broad differences within

the same sample were similarly reported for bare CdSe/ZnS QDs,[19] as therein described by so-called bleaching times, all in all suggesting a higher uniformity of the surface of our sample upon S growth.

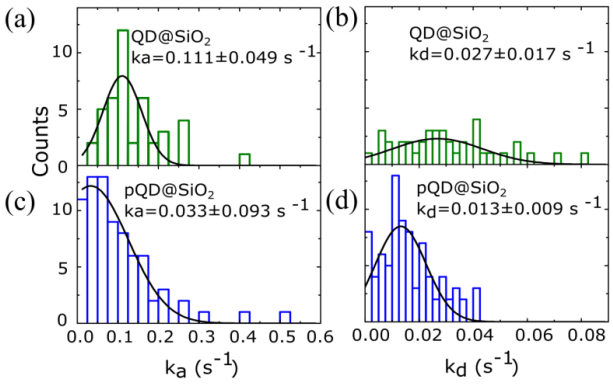

Figure 5. Statistical distributions of the activation and bleaching rates (k_a and k_d) for QD@SiO_2, (*a*) and (*b*), and pQD@SiO_2 clusters, (*c*) and (*d*). Gaussian fits to experimental distributions with mean ± HWHM data are displayed.

Typical values of k_a and k_d obtained in drop-casting experiments for similar QD systems [35, 40] are compiled along with ours on Table 1. To the best of our knowledge, k_a and k_d have not been reported in alloyed QDs to date, and never directly in solution from an optical trap. As shown on this table, earlier reported data are comparable to ours despite both k_a and k_d were shown to be proportional to the excitation power.[35-36, 40] More in depth, data on QDs drop-casted on a surface were usually pumped with some kW cm^{-2} [19, 38, 40] in contrast to the herein used irradiation power, which is three orders of magnitude higher under our experimental conditions (see Experimental section).

Table 1. Photo-brightening, k_a, and photo-bleaching, k_d, rates for QDs based on CdSe and ZnS under several excitation conditions

Composition	Irradiance (kW cm^{-2})	$\lambda_{excitation}$ (nm)	Excitation method	k_a (s^{-1})	k_d (s^{-1})	Ref.
CdSe/ZnS	Not reported	435-692	One photon	0.04195-0.00066	0.04712-0.00219	[35]
CdSe/ZnS	0.5	457-514		0.032-0.115	0.006-0.013	[40]
CdSe/ZnS	1.2-12	488		0.081-1.3	0.0182- 0.182	[40]
Alloyed CdSeZnS QD@SiO_2	6.3×10^3	835	Two photons	0.111	0.027	This work
Alloyed CdSeZnS pQD@SiO_2	6.3×10^3	835		0.033	0.013	

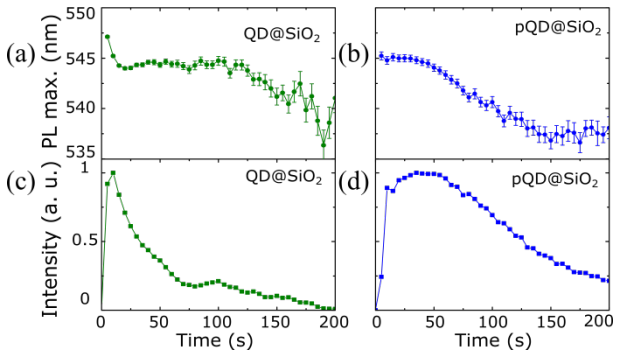

Figure 6. Emission peak shift, (*a*) and (*b*), and temporal evolution of the intensity, (*c*) and (*d*), for trapped QD clusters; (*a*) and (*c*), QD@SiO_2 and (*b*) and (*d*), pQD@SiO_2.

Wavelength-shifted PL signals have been measured during the luminescent evolution of both QD@SiO_2 and pQD@SiO_2 clusters and are represented in Fig. 6. The peak wavelength as a function of the time is shown in Figs. 6(*a*) and (*b*) for QD@SiO_2 and pQD@SiO_2 clusters, respectively. In the case of QD@SiO_2, after an initial blueshift (~2 nm), there appears a plateau followed by a longer blueshift (~5 nm). A blueshifted PL response may appear as a consequence of a light-driven element migration.[21, 41] The fact that the herein measured blueshift manifests with concomitant PL decrease, Fig. 6 (*c*), further indicates photo-oxidation,[42] which is expected due to the nature of the SiO_2 shell and the use of both ethanol as the dispersive medium and high photon fluxes. In contrast, in pQD@SiO_2 clusters though exhibiting a similar total blueshifted PL signal (by ~7 nm), the evolution of this spectral displacement and the associated intensity, Fig. 6 (d), is more gradual than for the QD@SiO_2 clusters.

It is remarkable that the PL signal is almost completely quenched after the first 50 seconds for the QD@SiO_2 clusters, Fig. 6 (*c*), whereas pQD@SiO_2 ones do not cease emitting by that time, Fig. 6 (*d*). The fact that the intensity decreases more slowly for pQD@SiO_2 than for QD@SiO_2 clusters implies that photo-oxidation is weaker for the former. Photo-oxidation may be attributed to an incomplete ZnS layer (with ZnS islands) on the surface of alloyed QDs, in which the

oxygen can diffuse, although other mechanisms such as charged species may be responsible for the less robust PL behavior of QD@SiO_2.[43]

All in all, the higher stability and performance in the optical trap exhibited by our pQD@SiO_2 hybrid system is attributed, firstly, to the graded shell in alloyed QDs, which has been proven to be less sensitive to oxygen than core/shell systems;[39] secondly, to the extra S layer providing better passivation; and thirdly, to the SiO_2 encapsulation, which increases protection of the QD surface from oxygen and other external reactants.[11, 44]

Conclusions

We studied the photo-brightening and bleaching dynamics of silica encapsulated QDs clusters for the first time in an optical trap and in solution. We found that the concurrence of alloyed QDs with both the use of an extra S layer and SiO_2 encapsulation tolerates irradiance doses three orders of magnitude higher than those reported for bare core/shell architectures on solid surfaces, which makes our QD systems and trapping scheme suggestive for tracking experiments in biological scenarios. We also found that although photo-oxidation is present in both QD@SiO_2 and pQD@SiO_2 systems, longer PL emission stability is registered for the latter, which is associated to the extra passivation S shell that attenuates or event suppresses other light-assisted bleaching mechanisms, in agreement with former qualitative studies with the QDs affixed on a solid surface.

ASSOCIATED CONTENT

Additional discussion on the inhomogeneously broadened emission of QD clusters and an example of multi-step, cumulative trapping. This material is available free of charge via the Internet at http://pubs.acs.org.

AUTHOR INFORMATION

Corresponding Author

*J. R. A.-G. ricardo.arias@imdea.org

*B. H. J. beatriz.hernandez@imdea.org,

Author Contributions

The manuscript was written through contributions of all authors. All authors have given approval to the final version of the manuscript.

Notes

Any additional relevant notes should be placed here.

ACKNOWLEDGMENT

The authors thank A. Blanco and D. Granados for fruitful discussion and S. de Lorenzo for technical help. H.R-R. is supported by an FPI-UAM fellowship and M. A. by a contract from Fundación IMDEA Nanociencia. The research leading to these results has received funding from the Spanish Ministry of Economy and Competitiveness (grant numbers MAT2015-71806-R and FIS2015-67367-C2-1-P), from Comunidad de Madrid (S2013/MIT-2740) and from UAM-Banco Santander (CEAL-AL/2015-15).

ABBREVIATIONS

QD quantum dot; OT optical trapping, NP nanoparticle, PL photoluminescence, NA numerical aperture, CCD charge-coupled device, PD photo-detector, PSD power spectrum density, PS polystyrene, LVDT linear variable differential transducer, XPS X-ray photoelectron spectroscopy, SILAR successive ionic layer adsorption and reaction, CER consecutive elementary reactions, HWHM half width at half maximum.

REFERENCES

(1) Bendix, P. M.; Jauffred, L.; Norregaard, K.; Oddershede, L. B. Optical Trapping of Nanoparticles and Quantum Dots. *IEEE J. Sel. Top. Quantum Electron.* **2014**, 20 (3), 4800112.

(2) Dienerowitz, M.; Mazilu, M.; Dholakia, K. Optical Manipulation of Nanoparticles: A Review. *J. Nanophotonics* **2008**, 2 (1), 021875–021875.

(3) Maragò, O. M.; Jones, P. H.; Gucciardi, P. G.; Volpe, G.; Ferrari, A. C. Optical Trapping and Manipulation of Nanostructures. *Nat. Nanotechnol.* **2013**, 8 (11), 807–819.

(4) Arias-González, J. R.; Nieto-Vesperinas, M. Optical Forces on Small Particles: Attractive and Repulsive Nature and Plasmon-Resonance Conditions. *J. Opt. Soc. Am. A* **2003**, 20 (7), 1201–1209.

(5) Arias-González, J. R.; Nieto-Vesperinas, M. Radiation Pressure over Dielectric and Metallic Nanocylinders on Surfaces: Polarization Dependence and Plasmon Resonance Conditions. *Opt. Lett.* **2002**, 27 (24), 2149–2151.

(6) Pan, L.; Ishikawa, A.; Tamai, N. Detection of Optical Trapping of CdTe Quantum Dots by Two-Photon-Induced Luminescence. *Phys. Rev. B* **2007**, 75 (16), 161305(R).

(7) Jauffred, L.; Oddershede, L. B. Two-Photon Quantum Dot Excitation during Optical Trapping. *Nano Lett.* **2010**, 10, 1927–1930.

(8) Jauffred, L.; Richardson, A. C.; Oddershede, L. B. Three-Dimensional Optical Control of Individual Quantum Dots. *Nano Lett.* **2008**, 8 (10), 3376–3380.

(9) Hormeño, S.; Gregorio-Godoy, P.; Pérez-Juste, J.; Liz-Marzán, L. M.; Juárez, B. H.; Arias-Gonzalez, J. R. Laser Heating Tunability by off-Resonant Irradiation of Gold Nanoparticles. *Small* **2014**, 10 (2), 376–384.

(10) Jensen, R. a.; Huang, I.-C.; Chen, O.; Choy, J. T.; Bischof, T. S.; Loncar, M.; Bawendi, M. G. Optical Trapping and Two-Photon Excitation of Colloidal Quantum Dots Using Bowtie Apertures. *ACS Photonics* **2016**, 3 (3), 423–427.

(11) Selvan, S. T.; Tan, T. T.; Ying, J. Y. Robust, Non-Cytotoxic, Silica-Coated CdSe Quantum Dots with Efficient Photoluminescence. *Adv. Mater.* **2005**, 17 (13), 1620–1625.

(12) Tsuboi, Y.; Shoji, T.; Kitamura, N.; Takase, M.; Murakoshi, K.; Mizumoto, Y.; Ishihara, H. Optical Trapping of Quantum Dots Based on Gap-Mode-Excitation of Localized Surface Plasmon. *J. Phys. Chem. Lett.* **2010**, 1 (15), 2327–2333.

(13) Fan, Y.; Helin, L.; Rongcheng, H.; Lu, H.; Hao, S.; Yinlin, S.; Yuqiang, J. Extremely High Brightness from Polymer-Encapsulated Quantum Dots for Two-Photon Cellular and Deep-Tissue Imaging. *Sci. Rep.* **2015**, 5, 9908.

(14) Asami, H.; Abe, Y.; Ohtsu, T.; Kamiya, I.; Hara, M. Surface State Analysis of Photobrightening in CdSe Nanocrystal Thin Films. *J. Phys. Chem. B* **2003**, 107, 12566–12568.

(15) Chon, J. W. M.; Zijlstra, P.; Gu, M.; Van Embden, J.; Mulvaney, P. Two-Photon-Induced Photoenhancement of Densely Packed CdSe/ZnSe/ZnS Nanocrystal Solids and Its Application to Multilayer Optical Data Storage. *Appl. Phys. Lett.* **2004**, 85, 5514–5516.

(16) Javier, A.; Strouse, G. F. Activated and Intermittent Photoluminescence in Thin CdSe Quantum Dot Films. *Chem. Phys. Lett.* **2004**, 391, 60–63.

(17) Bao, H.; Gong, Y.; Li, Z.; Gao, M. Enhancement Effect of Illumination on the Photoluminescence of Water-Soluble CdTe Nanocrystals: Toward Highly Fluorescent CdTe/CdS Core-Shell Structure. *Chem. Mater.* **2004**, 16 (15), 3853–3859.

(18) Jiong, M.; Chen, J. Y.; Zhang, Y.; Wang, P. N.; Guo, J.; Yang, W. L.; Wang, C. C. Photochemical Instability of Thiol-Capped CdTe Quantum Dots in Aqueous Solution and Living Cells: Process and Mechanism. *J. Phys. Chem. B* **2007**, 111, 12012–12016.

(19) Van Sark, W. G. J. H. M.; Frederix, P. L. T. M.; Bol, A. a.; Gerritsen, H. C.; Meijerink, A. Blueing, Bleaching, and Blinking of Single CdSe/ZnS Quantum Dots. *ChemPhysChem* **2002**, 3, 871–879.

(20) Acebrón, M.; Galisteo-López, J. F.; Granados, D.; López-Ogalla, J.; Gallego, J. M.; Otero, R.; López, C.; Juárez, B. H. Protective Ligand Shells for Luminescent SiO_2-Coated Alloyed Semiconductor Nanocrystals. *ACS Appl. Mater. Interfaces* **2015**, 7 (12), 6935-6945.

(21) Panda, S. K.; Hickey, S. G.; Waurisch, C.; Eychmüller, A. Gradated Alloyed CdZnSe Nanocrystals with High Luminescence Quantum Yields and Stability for Optoelectronic and Biological Applications. *J. Mater. Chem.* **2011**, 21, 11550–11555.

(22) Chen, O.; Zhao, J.; Chauhan, V. P.; Cui, J.; Wong, C.; Harris, D. K.; Wei, H.; Han, H.-S.; Fukumura, D.; Jain, R. K.; et al. Compact High-Quality CdSe-CdS Core-Shell Nanocrystals with Narrow Emission Linewidths and Suppressed Blinking. *Nat. Mater.* **2013**, 12 (5), 445–451.

(23) Ma, J.; Chen, J.-Y.; Guo, J.; Wang, C. C.; Yang, W. L.; Xu, L.; Wang, P. N. Photostability of Thiol-Capped CdTe Quantum Dots in Living Cells: The Effect of Photo-Oxidation. *Nanotechnology* **2006**, 17, 2083–2089.

(24) Cordero, S. R.; Carson, P. J.; Estabrook, R. A.; Strouse, G. F.; Buratto, S. K. Photo-Activated Luminescence of CdSe Quantum Dot Monolayers. *J. Phys. Chem. B* **2000**, 104, 12137–12142.

(25) Ristov, M.; Sinadinovski, G.; Grozdanov, I.; Mitreski, M. Chemical Deposition of TIN(II) Sulphide Thin Films. *Thin Solid Films* **1989**, 173 (1), 53–58.

(26) Smith, S. B.; Cui, Y.; Bustamante, C. Optical-Trap Force Transducer That Operates by Direct Measurement of Light Momentum. *Methods Enzymol.* **2003**, 361, 134–162.

(27) Hormeño, S.; Ibarra, B.; Chichón, F. J.; Habermann, K.; Lange, B. M. H.; Valpuesta, J. M.; Carrascosa, J. L.; Arias-Gonzalez, J. R. Single Centrosome Manipulation Reveals Its Electric Charge and Associated Dynamic Structure. *Biophys. J.* **2009**, 97 (4), 1022–1030.

(28) Hormeño, S.; Bastús, N. G.; Juárez, B. H.; Pietsch, A.; Weller, H.; Arias-Gonzalez, J. R. Plasmon-Exciton Interactions on Single Thermoresponsive Platforms Demonstrated by Optical Tweezers. *Nano Lett.* **2011**, No. 11, 4742–4747.

(29) Hosokawa, C.; Yoshikawa, H.; Masuhara, H. Cluster Formation of Nanoparticles in an Optical Trap Studied by Fluorescence Correlation Spectroscopy. *Phys. Rev. E* **2005**, 72 (2), 021408.

(30) Chiang, W.; Okuhata, T.; Usman, A.; Tamai, N.; Masuhara, H. Efficient Optical Trapping of CdTe Quantum Dots by Femtosecond Laser Pulses. *J. Phys. Chem. B* **2014**, 118 (49),

14010–14016.

(31) Bernal, J. D.; Mason, J. Packing of Spheres: Co-Ordination of Randomly Packed Spheres. *Nature* **1960**, 188 (4754), 910–911.

(32) Bormuth, V.; Jannasch, A.; Ander, M.; van Kats, C. M.; van Blaaderen, A.; Howard, J.; Schäffer, E. Optical Trapping of Coated Microspheres. *Opt. Express* **2008**, 16 (18), 13831–13844.

(33) Rohrbach, A. Stiffness of Optical Traps: Quantitative Agreement between Experiment and Electromagnetic Theory. *Phys. Rev. Lett.* **2005**, 95, 168102.

(34) Lee, S. F.; Osborne, M. a. Photodynamics of a Single Quantum Dot: Fluorescence Activation, Enhancement, Intermittency, and Decay. *J. Am. Chem. Soc.* **2007**, 129, 8936–8937.

(35) Shi, X.; Tu, Y.; Liu, X.; Yeung, E. S.; Gai, H. Photobleaching of Quantum Dots by Non-Resonant Light. *Phys. Chem. Chem. Phys.* **2013**, 15, 3130–3132.

(36) Galisteo-Lopez, J. F.; Anaya, M.; Calvo, M. E.; Miguez, H. Environmental Effects on the Photophysics of Organic-Inorganic Halide Perovskites. *J. Phys. Chem. Lett.* **2015**, 6, 2200–2205.

(37) Borowicz, P.; Hotta, J.; Sasaki, K.; Masuhara, H. Chemical and Optical Mechanism of Microparticle Formation of poly(N-Vinylcarbazole) in N,N-Dimethylformamide by Photon Pressure of a Focused near-Infrared Laser Beam. *J. Phys. Chem. B* **1998**, 102 (11), 1896–1901.

(38) Van Sark, W. G. J. H. M.; Frederix, P. L. T. M.; Van den Heuvel, D. J.; Gerritsen, H. C.; Bol, A. A.; Van Lingen, J. N. J.; De Mello Donegá, C.; Meijerink, A. Photooxidation and Photobleaching of Single CdSe/ZnS Quantum Dots Probed by Room-Temperature Time-Resolved Spectroscopy. *J. Phys. Chem. B* **2001**, 105, 8281–8284.

(39) Wang, Y.; Tang, Z.; Correa-duarte, M. A.; Pastoriza-santos, I.; Giersig, M.; Kotov, N. A.; Liz-Marzán, L. M. Mechanism of Strong Luminescence Photoactivation of Citrate-Stabilized Water-Soluble Nanoparticles with CdSe Cores. *J. Phys. Chem. B* **2004**, 108, 15461–15469.

(40) Osborne, M. a.; Lee, S. F. Quantum Dot Photoluminescence Activation and Decay: Dark, Bright, and Reversible Populations in ZnS-Capped CdSe Nanocrystals. *ACS Nano* **2011**, 5 (10), 8295–8304.

(41) Xia, X.; Liu, Z.; Du, G.; Li, Y.; Ma, M. Structural Evolution and Photoluminescence of Zinc-Blende CdSe-Based CdSe/ZnS Nanocrystals. *J. Phys. Chem. C* **2010**, 114 (32), 13414–13420.

(42) Spanhel, L.; Haase, M.; Weller, H.; Henglein, A. Photochemistry of Colloidal Semiconductors. 20. Surface Modification and Stability of Strong Luminescing CdS Particles. *J. Am. Chem. Soc.* **1987**, 109 (19), 5649–5655.

(43) Darbandi, M.; Urban, G.; Krüger, M. A Facile Synthesis Method to Silica Coated CdSe/ZnS Nanocomposites with Tuneable Size and Optical Properties. *J. Colloid Interface Sci.* **2010**, 351 (1), 30–34.

(44) Pietra, F.; van Dijk - Moes, R. J. A.; Ke, X.; Bals, S.; Van Tendeloo, G.; de Mello Donega, C.; Vanmaekelbergh, D. Synthesis of Highly Luminescent Silica-Coated CdSe/CdS Nanorods. *Chem. Mater.* **2013**, 25 (17), 3427–3434.

TOC graphic